Crystal structure of pemetrexed disodium heptahydrate, $C_{20}H_{33}N_5Na_2O_{13}$ (Alimta)

James A. Kaduk,[1,a)] Amy M. Gindhart,[2] and Thomas N. Blanton[2]
[1]*Illinois Institute of Technology, 3101 S. Dearborn St., Chicago IL 60616, and North Central College, 30 N. Brainard St., Naperville IL 60540*
[2]*ICDD, 12 Campus Blvd., Newtown Square PA, 19073-3273*

(Received 30 July 2017; accepted 8 January 2018)

The crystal structure of pemetrexed disodium heptahydrate has been solved and refined using synchrotron X-ray powder diffraction data, and optimized using density functional techniques. Pemetrexed disodium heptahydrate crystallizes in space group $P2_1$ (#4) with $a = 11.732\,697(27)$, $b = 5.244\,195(14)$, $c = 21.689\,00(6)$ Å, $\beta = 92.663\,90(20)^{\circ}$, $V = 1333.051(6)$ Å^3, and $Z = 2$. Each of the two ionized carboxylate groups acts as a unidentate ligand to a Na cation. The remaining five positions of the octahedral coordination spheres are occupied by water molecules. The Na octahedra share an edge to form pairs. These pairs share corners to form chains along the *b*-axis. All of the water molecule hydrogen atoms act as hydrogen bond donors. In addition the hydrogen atoms associated with the nitrogen atoms and amino groups of the pemetrexed anion were also observed to act as hydrogen bond donors. The powder pattern has been submitted to the International Centre for Diffraction Data (ICDD) for inclusion in the Powder Diffraction File™.
 [doi:10.1017/S0885715618000179]

Key words: pemetrexed disodium heptahydrate, powder diffraction, Rietveld refinement, density functional theory

I. INTRODUCTION

Pemetrexed (brand name Alimta) is a chemotherapy drug manufactured and marketed by Eli Lilly and Company. It is used for the treatment of pleural mesothelioma and non-small cell lung cancer. In a group of chemotherapy drugs referred to as folate antimetabolites, Pemetrexed prevents RNA and DNA formation in cancer, as well as normal, cells. Pemetrexed is often administered in combination with cisplatin. The systematic name (CAS Registry number 357166-29-1) for the sodium salt heptahydrate of Pemetrexed is (2S)-2-[[4-[2-(2-amino-4-oxo-1,7-dihydropyrrolo[2,3-d]pyrimidin-5-yl)ethyl] benzoyl]amino]pentanedioate, disodium salt heptahydrate. A two-dimensional molecular diagram of the pemetrexed dianion is shown in Figure 1.

This work was carried out as part of a project (Kaduk *et al.*, 2014) to determine the crystal structures of large-volume commercial pharmaceuticals, and include high-quality powder diffraction data for them in the Powder Diffraction File (ICDD, 2016).

II. EXPERIMENTAL

Pemetrexed disodium heptahydrate was a commercial regent, purchased from US Pharmacopeia (Lot #F042E0), and was used as-received. The white powder was packed into a 1.5 mm diameter Kapton capillary, and rotated during the measurement at ~50 cycles s^{-1}. The powder pattern was measured at 295 K at beam line 11-BM (Lee *et al.*, 2008; Wang *et al.*, 2008) of the Advanced Photon Source at Argonne National Laboratory using a wavelength of 0.414 533 Å from 0.5–50° 2θ with a step size of 0.001° and a counting time of 0.1 s step^{-1}. The pattern was indexed on a primitive monoclinic unit cell having $a = 11.732$, $b = 5.244$, $c = 21.687$ Å, $\beta = 92.7°$, $V = 1332.7$ Å^3, and $Z = 2$ using Jade (MDI, 2016). Analysis of the systematic absences using EXPO2014 (Altomare *et al.*, 2013) suggested the space group $P2_1$, which was confirmed by successful solution and refinement of the structure. A reduced cell search in the Cambridge Structural Database (Groom *et al.*, 2016) combined with the chemistry "C H N Na O only" yielded 2 hits for MOF-706, but no structure for pemetrexed or related phases.

A pemetrexed molecule was built using Spartan '16 (Wavefunction, 2017), and its equilibrium conformation determined. The minimum energy conformation was more compact than is observed in the solid state. The resulting .mol2 file was converted into a Fenske-Hall Z-matrix file using OpenBabel (O'Boyle *et al.*, 2011). Initial attempts to solve the structure (with several programs) using the pemetrexed molecule, 2 Na atoms, and 7 O atoms as fragments were unsuccessful. Under the assumption that the Na coordination was octahedral, a pemetrexed and two NaO_6 octahedra (Na-O = 2.46 Å) were used as fragments to solve the structure with FOX (Favre-Nicolin and Černý, 2002). The maximum sinθ/λ used in the structure solution was 0.33 Å^{-1}. The Dynamical Occupancy Correction option indicated some overlapping oxygen atoms, but several others had to be removed manually.

Rietveld refinement was carried out using GSAS (Toby, 2001; Larson and Von Dreele, 2004). Only the 1.0–25.0° portion of the pattern was included in the refinement ($d_{min} = 0.957$ Å),

a)Author to whom correspondence should be addressed. Electronic mail: kaduk@polycrystallography.com

with an excluded region 1.2–1.9° 2θ to eliminate a relatively sharp peak from the Kapton capillary. All non-H bond distances and angles were subjected to restraints, based on a Mercury/Mogul Geometry Check (Bruno *et al.*, 2004; Sykes *et al.*, 2011) of the molecule. The Mogul average and standard deviation for each quantity were used as the restraint parameters. The N1-N9/C12/C13/N15/C17 and C23-C28 portions of the molecule were restrained to be planar. The Na-O distances were not restrained. The restraints contributed 11.2% to the final χ^2. The U_{iso} of each hydrogen atom was fixed at 1.3 × that of the heavy atom to which it was attached. The peak profiles were described using profile function #4 (Thompson *et al.*, 1987; Finger *et al.*, 1994), which includes the Stephens (1999) anisotropic strain broadening model. The background was modeled using a 3-term shifted Chebyshev polynomial, with a 12-term diffuse scattering function to model the Kapton capillary and any amorphous component. The final refinement of 162 variables using 23 371 observations (23 301 data points and 170 restraints) yielded the residuals $Rwp = 0.0783$, $Rp = 0.0635$, and $\chi^2 = 1.315$. The largest peak (1.54 Å from C2) and hole (1.78 Å from C17) in the difference Fourier map were 0.37 and $-0.26\ e\text{Å}^{-3}$, respectively. The Rietveld plot is included as Figure 2. The largest errors in the fit are in the shapes of some of the low-angle peaks.

A density functional geometry optimization (fixed experimental unit cell) was carried out using CRYSTAL14 (Dovesi *et al.*, 2014). The basis sets for the H, C, N, O, and Na atoms were those of Peintinger *et al.* (2013). The calculation was run on eight 2.1 GHz Xeon cores (each with 6 Gb RAM) of a 304-core Dell Linux cluster at IIT, used 8 *k*-points and the B3LYP functional, and took ~24 days.

III. RESULTS AND DISCUSSION

The observed powder pattern is similar to Figure 1 of US Patent Application Publication 2003/0216416 (Figure 3, digitized using UN-SCAN-IT 7.0 (Silk Scientific, 2013)) to conclude that this sample is the same "heptahydrate crystalline salt" of pemetrexed disodium as that claimed by Eli Lilly and Company (Chelius *et al.*, 2003). Other crystalline forms and hydrates have been reported. The refined atom coordinates of pemetrexed disodium heptahydrate and the coordinates from the density functional theory (DFT) optimization of this study are reported in the Crystallographic Information Framework attached as Supplementary Material. The root-mean-square deviation of the non-hydrogen atoms in the pemetrexed anions is 0.152 Å (Figure 4). The maximum

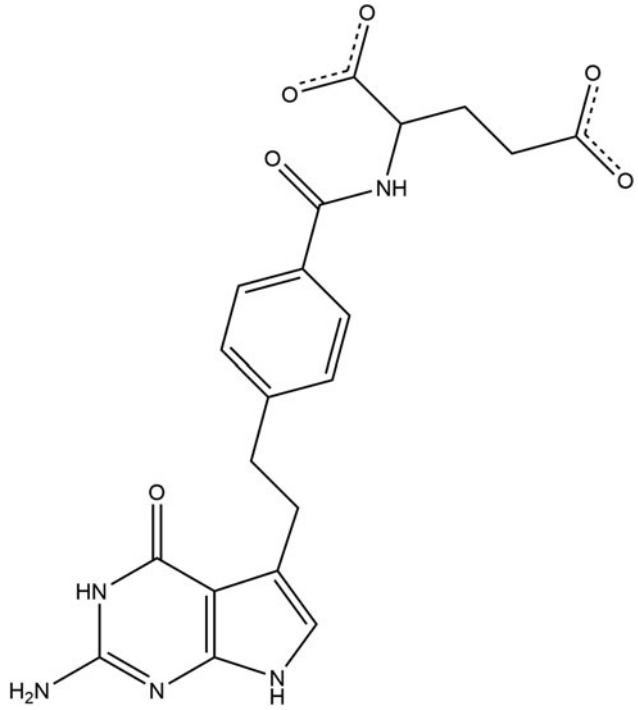

Figure 1. The molecular structure of the pemetrexed dianion.

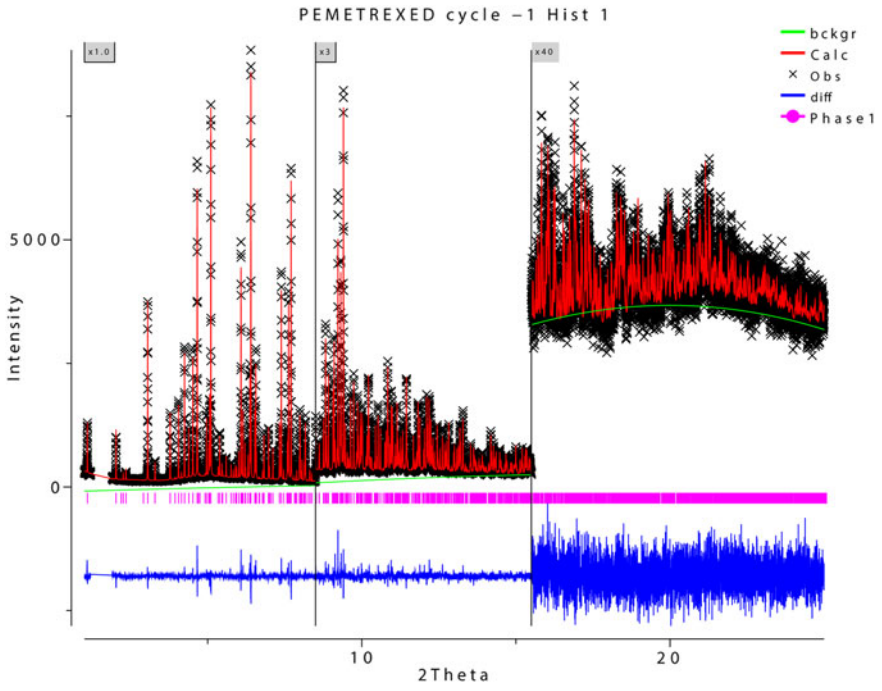

Figure 2. (Colour online) The Rietveld plot for the refinement of pemetrexed disodium heptahydrate. The black crosses represent the observed data points, and the red line is the calculated pattern. The blue curve is the difference pattern, plotted at the same vertical scale as the other patterns. The vertical scale has been multiplied by a factor of 3 for $2\theta > 8.0°$, and by a factor of 40 for $2\theta > 16.0°$.

https://doi.org/10.1017/S0885715618000179 Published online by Cambridge University Press

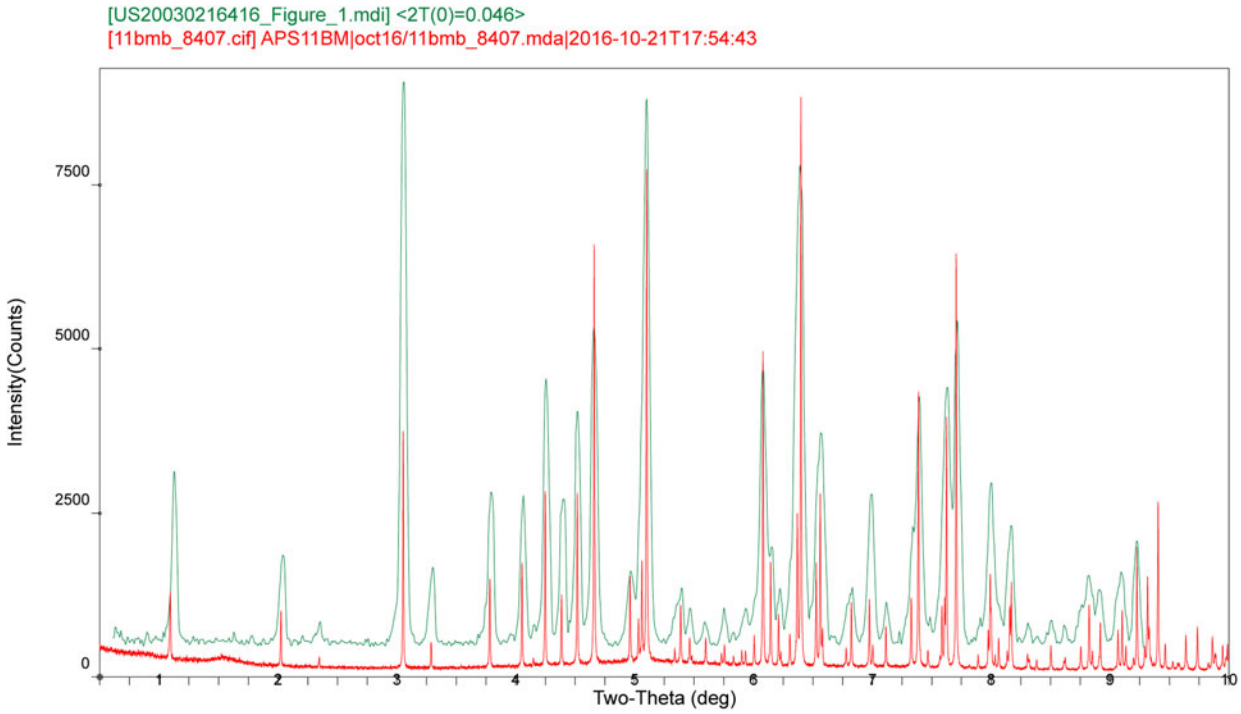

Figure 3. (Colour online) Comparison of the powder pattern of pemetrexed disodium heptahydrate to the pattern of Figure 1 of US Patent Application 2003/0216416 for the "heptahydrate crystalline salt" of pemetrexed disodium claimed by Eli Lilly and Company.

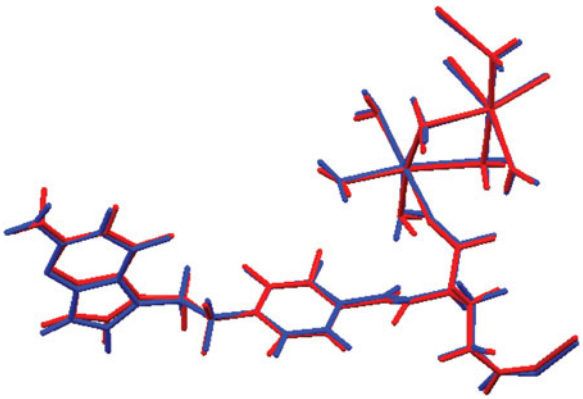

Figure 4. (Colour online) Comparison of the refined and optimized structures of pemetrexed disodium heptahydrate. The Rietveld refined structure is in red, and the DFT-optimized structure is in blue.

deviation is 0.295 Å, at N9. The good agreement between the refined and optimized structures is evidence that the experimental structure is correct (van de Streek and Neumann, 2014). This discussion uses the DFT-optimized structure. The asymmetric unit (with atom numbering) is illustrated in Figure 5, and the crystal structure is presented in Figure 6.

Almost all of the bond distances, bond angles, and torsion angles in the pemetrexed anion fall within the normal ranges indicated by a Mercury Mogul Geometry check (Macrae *et al.*, 2008). The C12-C4-C3 (optimized = 107.9°, average = 112.6(12)°, Z-score = 3.96), and O49-C48-C37 (optimized = 119.7°, average = 111.5(27)°, Z-score = 3.01) are flagged as unusual. The torsion angles C25-C23-C20-C17, C26-C23-C20-C17, and O46-C45-C42-C32 are flagged as unusual. Although these lie away from the peaks in the distributions, the distributions of these torsion angles cover all

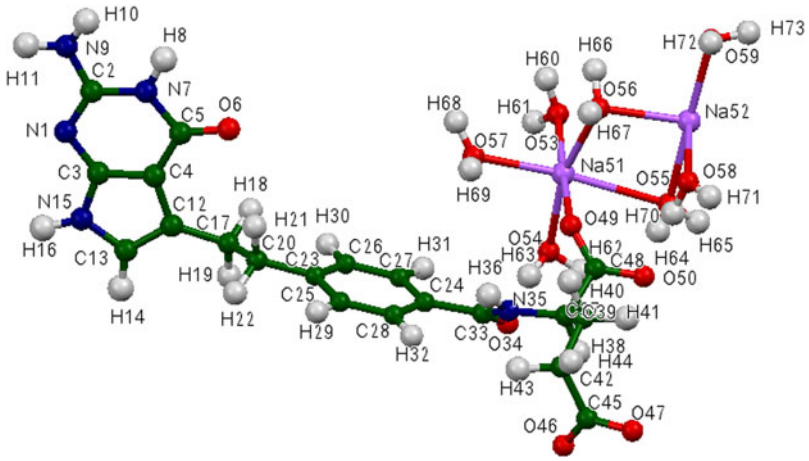

Figure 5. (Colour online) The asymmetric unit of pemetrexed disodium heptahydrate, with the atom numbering. The atoms are represented by 50% probability spheroids.

https://doi.org/10.1017/S0885715618000179 Published online by Cambridge University Press

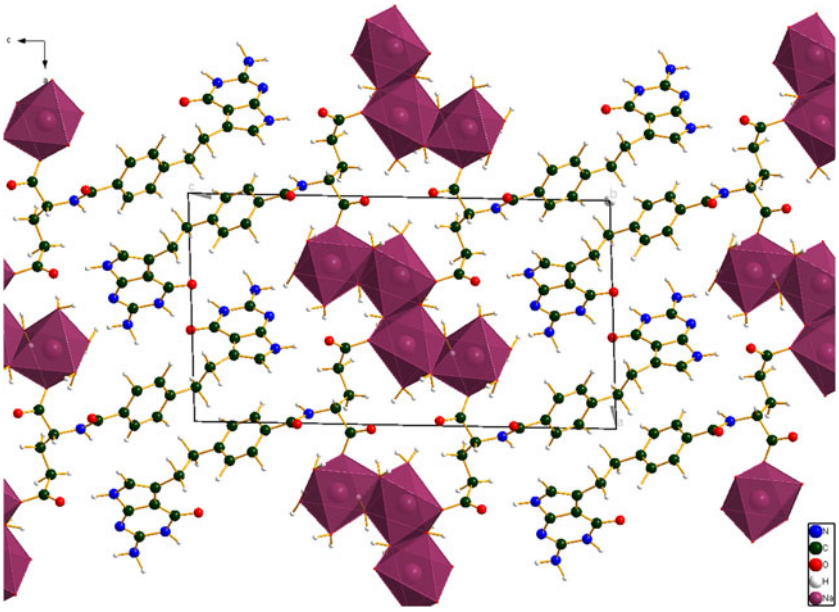

Figure 6. (Colour online) The crystal structure of pemetrexed disodium heptahydrate, viewed down the *b*-axis.

possible values, and the ones here occur in the lower-probability regions of the distributions.

Each ionized carboxylate group acts as a unidentate ligand to a Na cation. The remaining five positions of the octahedral coordination spheres are occupied by water molecules. The Na51 and Na52 octahedra share an edge (the water molecules O55 and O56) to form pairs. These pairs share corners (the water molecule O59) to form chains along the *b*-axis. All of the water molecules are coordinated to at least one Na. The bond valence sums of Na51 and Na52 are 1.12 and 1.13, respectively. The atomic charges and Mulliken overlap populations indicate that the Na-O bonding is primarily ionic, but that the bonds have significant covalent character. The overlap populations range from 0.03 to 0.06 *e*.

Quantum chemical geometry optimizations (Hartree-Fock/6-31G*/water) using Spartan '16 (Wavefunction, 2017) indicated that the observed conformation of the pemetrexed dianion in pemetrexed disodium heptahydrate is 16.6 kcal mole^{-1} higher in energy than a local minimum. A molecular mechanics conformational analyses indicated that the global minimum energy conformation is more compact (with parallel rings), and thus intermolecular interactions are important in determining the solid-state conformation.

Analysis of the contributions to the total crystal energy using the Forcite module of Materials Studio (Dassault, 2014) suggests that bond angle distortion terms are significant in the intramolecular deformation energy. The intermolecular energy is dominated by electrostatic attractions, which in this force-field-based analysis include hydrogen bonds. The hydrogen bonds are better analyzed using the results of the DFT calculation.

As expected, there is an extensive array of hydrogen bonds (Table I). All of the water molecule hydrogen atoms (H60-H73) act as hydrogen bond donors. Six of these 14 hydrogen bonds form to other water molecules. The oxygen atoms of the ionized carboxylate groups (O46, O47, O49, and O50) act as acceptors, as do the carbonyl oxygen O34 and the ring nitrogen N1. The energies of the O-H···O

TABLE I. Hydrogen bonds in pemetrexed disodium heptahydrate.

H-Bond	D-H, Å	H···A, Å	D···A, Å	D-H···Å	Overlap, *e*	Energy, kcal mol^{-1}
O59-H73···O53	0.975	1.972	2.886	155.3	0.041	11.1
O59-H72···O47	0.988	1.750	2.730	171.4	0.058	13.2
O58-H71···O50	0.983	1.866	2.834	167.5	0.058	13.2
O58-H70···O50	0.980	1.912	2.891	177.0	0.048	12.0
O57-H69···O54	0.982	1.850	2.779	156.9	0.062	13.6
O57-H68···N1	0.975	1.996	2.938	161.7	0.038	
O56-H67···O55	0.971	2.126	3.034	154.8	0.033	9.9
O56-H66···O47	0.978	1.879	2.832	164.0	0.042	11.2
O55-H65···O58	0.989	1.771	2.759	175.9	0.068	14.3
O55-H64···O50	0.984	1.849	2.828	173.2	0.056	12.9
O54-H63···O34	0.978	1.840	2.799	166.3	0.046	11.7
O54-H62···O49	0.984	1.793	2.752	163.8	0.057	13.0
O53-H61···N1	0.974	2.288	3.237	164.3	0.036	
O53-H60···O46	0.991	1.705	2.695	176.8	0.064	13.8
N35-H36···O34	1.015	2.259	3.264	170.1	0.028	
N15-H16···O46	1.032	1.694	2.717	170.4	0.080	
N9-H11···O57	1.013	2.067	2.934	142.2	0.029	
N7-H8···O6	1.036	1.678	2.712	174.8	0.077	

https://doi.org/10.1017/S0885715618000179 Published online by Cambridge University Press

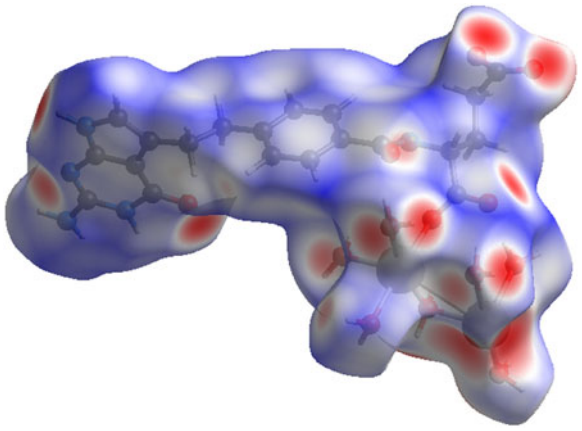

Figure 7. (Colour online) The Hirshfeld surface of pemetrexed disodium heptahydrate. Intermolecular contacts longer than the sums of the van der Waals radii are colored blue, and contacts shorter than the sums of the radii are colored red. Contacts equal to the sums of radii are white.

hydrogen bonds were calculated from the Mulliken overlap populations by the correlation in Rammohan and Kaduk (2017). In addition, the ring nitrogen atoms N15-H16 and N7-H8 act as hydrogen bond donors to carboxylate oxygen atom O46 and the carbonyl oxygen O6. The graph sets (Etter, 1990; Bernstein *et al.*, 1995; Shields *et al.*, 2000) for these hydrogen bonds are *C1,1(17)* and *C1,1(4)* respectively. The secondary amino group H35-H36 acts as a donor to the carbonyl oxygen O34, with graph-set *C1,1(4)*. The primary amino group N9-H11 acts as a donor to the water molecule O57, with graph-set *C1,1(20)*. Despite an apparently favorable geometry, the Mulliken overlap populations indicate that hydrogen H10 does not participate in a hydrogen bond.

The volume enclosed by the Hirshfeld surface (Figure 7; Hirshfeld, 1977; McKinnon *et al.*, 2004; Spackman and Jayatilaka, 2009; Wolff *et al.*, 2012) is 653.59 Å^3, 98.0% of 1/2 the unit cell volume. The molecules are thus not tightly packed. All of the significant close contacts (red in Figure 7) involve the hydrogen bonds.

The Bravais-Friedel-Donnay-Harker (Bravais, 1866; Friedel, 1907; Donnay and Harker, 1937) morphology suggests that we might expect platy morphology for pemetrexed disodium heptahydrate, with {001} as the principal faces, or needle morphology with {010} as the long axis. A 4th-order spherical harmonic preferred orientation model was included in the refinement; the texture index was only 1.007, indicating that preferred orientation was not significant in this rotated capillary specimen. The powder pattern of pemetrexed disodium heptahydrate has been submitted to ICDD for inclusion in the Powder Diffraction File.

SUPPLEMENTARY MATERIAL

The supplementary material for this article can be found at https://doi.org/10.1017/S0885715618000179.

ACKNOWLEDGEMENTS

Use of the Advanced Photon Source at Argonne National Laboratory was supported by the U S Department of Energy, Office of Science, Office of Basic Energy Sciences, under Contract No. DE-AC02-06CH11357. This work was partially supported by the International Centre for Diffraction Data. The authors thank Lynn Ribaud for his assistance in data collection, and Andrey Rogachev for the use of computing resources at IIT.

Altomare, A., Cuocci, C., Giacovazzo, C., Moliterni, A., Rizzi, R., Corriero, N., and Falcicchio, A. (**2013**). "EXPO2013: a kit of tools for phasing crystal structures from powder data," J. Appl. Crystallogr. **46**, 1231–1235.

Bernstein, J., Davis, R. E., Shimoni, L., and Chang, N. L. (**1995**). "Patterns in hydrogen bonding: functionality and graph set analysis in crystals," Angewandte Chem. Int. Ed. Eng. **34**(15), 1555–1573.

Bravais, A. (**1866**). *Etudes Cristallographiques* (Gauthier Villars, Paris).

Bruno, I. J., Cole, J. C., Kessler, M., Luo, J., Motherwell, W. D. S., Purkis, L. H., Smith, B. R., Taylor, R., Cooper, R. I., Harris, S. E., and Orpen, A. G. (**2004**). "Retrieval of crystallographically-derived molecular geometry information," J. Chem. Inf. Sci. **44**, 2133–2144.

Chelius, E. C., Reutzel-Eden, S. M., and Snorek, S. V. (**2003**). "Novel Crystalline of N-[4-[2-(amino-4,7-dihydro-4-oxo-3H-pyrrolo[2,3-D]pyrimidin-5-yl)ethyl]-benzoyl]-L-glutamic acid and Process Therefore," US Patent Application 2003/0216416.

Dassault Systèmes (**2014**). *Materials Studio* 8.0 (BIOVIA, San Diego, CA).

Donnay, J. D. H., and Harker, D. (**1937**). "A new law of crystal morphology extending the law of Bravais," Amer. Mineral. **22**, 446–467.

Dovesi, R., Orlando, R., Erba, A., Zicovich-Wilson, C. M., Civalleri, B., Casassa, S., Maschio, L., Ferrabone, M., De La Pierre, M., D-Arco, P., Noël, Y., Causà, M., Kirtman, B. (**2014**). "CRYSTAL14: a program for the ab initio investigation of crystalline solids," Int. J. Quantum Chem. **114**, 1287–1317.

Etter, M. C. (**1990**). "Encoding and decoding hydrogen-bond patterns of organic compounds," Acc. Chem. Res. **23**(4), 120–126.

Favre-Nicolin, V., and Černý, R. (**2002**). FOX, "free objects for crystallography: a modular approach to ab initio structure determination from powder diffraction," J. Appl. Crystallogr. **35**, 734–743.

Finger, L. W., Cox, D. E., and Jephcoat, A. P. (**1994**). "A correction for powder diffraction peak asymmetry due to axial divergence," J. Appl. Crystallogr. **27**(6), 892–900.

Friedel, G. (**1907**). "Etudes sur la loi de Bravais," Bull. Soc. Fr. Mineral. **30**, 326–455.

Groom, C. R., Bruno, I. J., Lightfoot, M. P., and Ward, S. C. (**2016**). "The cambridge structural database," Acta Crystallogr. Sect. B: Struct. Sci., Cryst. Eng. Mater. **72**, 171–179.

Hirshfeld, F. L. (**1977**). "Bonded-atom fragments for describing molecular charge densities," Theor. Chem. Acta **44**, 129–138.

ICDD (**2016**). PDF-4+ 2016 (Database), edited by Dr. Soorya Kabekkodu, International Centre for Diffraction Data, Newtown Square, PA, USA.

Kaduk, J. A., Crowder, C. E., Zhong, K., Fawcett, T. G., and Suchomel, M. R. (**2014**). "Crystal structure of atomoxetine hydrochloride (Strattera), $C_{17}H_{22}NOCl$," Powder Diffr. **29**(3), 269–273.

Larson, A. C., and Von Dreele, R. B. (**2004**). *General Structure Analysis System,* (*GSAS*) (Report LAUR 86-784). Los Alamos National Laboratory.

Lee, P. L., Shu, D., Ramanathan, M., Preissner, C., Wang, J., Beno, M. A., Von Dreele, R. B., Ribaud, L., Kurtz, C., Antao, S. M., Jiao, X., and Toby, B. H. (**2008**). "A twelve-analyzer detector system for high-resolution powder diffraction," J. Synch. Rad. **15**(5), 427–432.

Macrae, C. F., Bruno, I. J., Chisholm, J. A., Edington, P. R., McCabe, P., Pidcock, E., Rodriguez-Monge, L., Taylor, R., van de Streek, J., and Wood, P. A. (**2008**). "Mercury CSD 2.0 – new features for the visualization and investigation of crystal structures," J. Appl. Crystallogr. **41**, 466–470.

McKinnon, J. J., Spackman, M. A., and Mitchell, A. S. (**2004**). "Novel tools for visualizing and exploring intermolecular interactions in molecular crystals," Acta Cryst. Sect. B **60**, 627–668.

MDI (**2016**). *Jade* 9.7 (Materials Data. Inc., Livermore, CA).

O'Boyle, N., Banck, M., James, C. A., Morley, C., Vandermeersch, T., and Hutchison, G. R. (**2011**). "Open Babel: an open chemical toolbox," J. Chem. Informatics **3**, 33. doi: 10.1186/1758-2946-3-33.

Peintinger, M. F., Vilela Oliveira, D., and Bredow, T. (**2013**). "Consistent Gaussian basis sets of triple-zeta valence with polarization quality for solid-state calculations," J. Comput. Chem. **34**, 451–459.

Rammohan, A., and Kaduk, J. A. (**2017**). "Crystal structures of alkali metal (group 1) citrate salts," Acta Cryst. Sect. B: Cryst. Eng. Mater. hw5048.
Shields, G. P., Raithby, P. R., Allen, F. H., and Motherwell, W. S. (**2000**). "The assignment and validation of metal oxidation states in the cambridge structural database," Acta Cryst. Sec. B: Struct. Sci. **56**(3), 455–465.
Silk Scientific (**2013**). *UN-SCAN-IT* 7.0 (Silk Scientific Corporation, Orem, UT).
Spackman, M. A., and Jayatilaka, D. (**2009**). "Hirshfeld surface analysis," CrystEngComm **11**, 19–32.
Stephens, P. W. (**1999**). "Phenomenological model of anisotropic peak broadening in powder diffraction," J. Appl. Crystallogr. **32**, 281–289.
Sykes, R. A., McCabe, P., Allen, F. H., Battle, G. M., Bruno, I. J., and Wood, P. A. (**2011**). "New software for statistical analysis of cambridge structural database data," J. Appl. Crystallogr. **44**, 882–886.
Thompson, P., Cox, D. E., and Hastings, J. B. (**1987**). "Rietveld refinement of Debye-Scherrer synchrotron X-ray data from Al_2O_3," J. Appl. Crystallogr. **20**(2), 79–83.
Toby, B. H. (**2001**). "EXPGUI, a graphical user interface for GSAS," J. Appl. Crystallogr. **34**, 210–213.
van de Streek, J., and Neumann, M. A. (**2014**). "Validation of molecular crystal structures from powder diffraction data with dispersion-corrected density functional theory (DFT-D)," Acta Cryst. Sect. B: Struct. Sci., Cryst. Eng. Mater. **70**(6), 1020–1032.
Wang, J., Toby, B. H., Lee, P. L., Ribaud, L., Antao, S. M., Kurtz, C., Ramanathan, M., Von Dreele, R. B., and Beno, M. A. (**2008**). "A dedicated powder diffraction beamline at the advanced photon source: commissioning and early operational results," Rev. Sci. Inst. **79**, 085105.
Wavefunction, Inc. (**2017**). *Spartan '16 Version 2.0.3* (Wavefunction Inc., Irvine, CA).
Wolff, S. K., Grimwood, D. J., McKinnon, M. J., Turner, M. J., Jayatilaka, D., and Spackman, M. A. (**2012**). *CrystalExplorer Version* 3.1 (Perth, Western Australia: University of Western Australia).

https://doi.org/10.1017/S0885715618000179 Published online by Cambridge University Press